Proceedings of the 2005 IEEE/ASME
International Conference on Advanced Intelligent Mechatronics
Monterey, California, USA, 24-28 July, 2005

An overview of the micro-manipulation system [*mü*]MAD

D. Sinan Haliyo, Gentiane Venture, Stéphane Régnier and Jean-Claude Guinot

***Abstract*— The micro-manipulation system developed in Laboratoire de Robotique de Paris (LRP) is described in this paper. This system, called [*mü*]MAD, is based on the use of adhesion forces and inertial effects for handling of objects which range from 1 to 100 . Moreover, enhanced user interaction is provided through a 6 dof haptic interface for force feedback remote handling. Some advanced features of [*mü*]MAD such as mechanical characterizations and sorting are also presented.**

***Index Terms*— Micro/nano manipulation, adhesion forces, force and vision servoing, haptic coupling.**

I. Introduction

Due to recent development of MEMS and biotechnology, there is a great demand for original micromanipulation techniques. Many approaches have been proposed to manipulate microscopic objects. The principal obstacle specific to this scale is that the force of gravity becomes negligible in comparison with adhesion forces. Consequently, any microsystem based on the miniaturisation of conventional macroscopic robots encounters a lot of difficulties in releasing a gripped object as it adheres to the gripper. Complex techniques are thus necessary to reduce adhesion, such as electrostatic detachment [1].

Whatever the employed techniques (with contact or not), and the environment (in air, liquid or vacuum) [2], due to specific mechanical and physical laws which govern the micro-world, micromanipulation systems often suffer from a lack of reproducibility. That is why micromanipulation tasks need complex and robust control based on sensor feedback.

An original approach has been developed at LRP. Contrary to the general "adhesionless" approach, it is based on the use of adhesion forces for gripping, as stated in our earlier works [3]. The release is achieved through inertial effects [4] or by rolling [5]. This paper gives an overview of the theoretical approach for the manipulation by adhesion and then describes our prototype manipulator [*mü*]MAD. Implemented force and vision control schemes are also presented, along with the homothetic coupling with an haptic interface, which guarantees unconditional stability. At last, some experimental results are presented.

II. Theoretical Analysis

The adhesion phenomena is mainly a result of intermolecular potentials, as expressed by Van der Waals forces [6]. Capillarity and electrostatic are also environment-dependent forces that contribute to the adhesion. A theoretical study of these forces are presented in our earlier works [7].

Authors are with the Laboratoire de Robotique de Paris, Univ. Paris 6 - CNRS, BP 61, 92265 Fontenay aux Roses, France. mailto:{haliyo,regnier}@robot.jussieu.fr

For micro-scale objects, these forces have higher magnitudes than the gravitational force and they are mainly attractive. Nevertheless, they depend on the inverse square or cube of the distance between the surfaces, for example for Van der Waals, and their influence become obvious only in very short range (less then 100 nm). A minimum amount of force is thus necessary to separate two medium in contact. This force is commonly called "*pull-off*". In the case of a sphere (radius R) on planar surface, its expresion is approximately given by Johnson-Kendall-Roberts (for the lower boundary) or Derjaguin-Muller-Toporov (for the higher boundary) contact models [8], [9].

$$\frac{3}{2}\pi RW \leq F_{pull-off} \leq 2\pi RW \tag{1}$$

where W is the Van der Waals work of adhesion between the two medium.

Under these circumstances, it is clear that classical multi finger gripper architecture is not well adapted for micromanipulation, unless the adhesion could be considerably reduced, as the gripped objects stick to the gripper and the release is often hazardous. The reduction of adhesion can be achieved by choosing materials with weak Van der Waals potentials or by the use of rough surfaces but in most cases, it is not possible to guarantee a macroscale-like, i.e *adhesionless*, behaviour.

However, it is possible to take advantage of the adhesion for gripping, using a tool with high surface energy and low surface roughness. In this case, one can pick-up a microobject by simple contact. This approach is very interesting as it does not need a complex gripper architecture for grasping. The obvious problem in this case is the release, as it is necessary to overcome the adhesion between the gripping tool and the object. The use of the inertial force is a possible solution. To study its feasability, the dynamical analysis of the release task, including contact and adhesion forces, is performed.

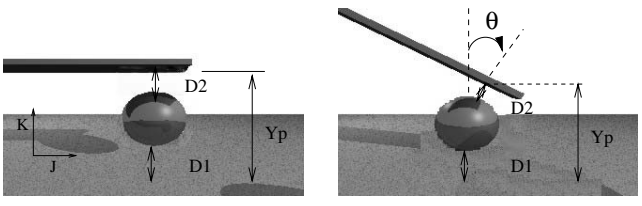

Fig. 1. Description of the micro-manipulation task

Simulations of the dynamic model show the existence of a value of initial acceleration $\ddot{Y}$ of the gripper over which inertial effects overbalance the adhesion between the tool

and the object, causing the release. This acceleration depends on both the mass of the object and the angle of slope θ of the gripper. A close examination of these simulation results lead to the conclusion that in order to achieve the release accurately, accelerations ranging from 10^4 to 10^6 are needed.

Another way to release a spherical object is by rolling. If one is able to control the contact force, it is possible to move the object to the extremity of the gripper by switching between the sliding and rolling modes. Once on the boundary of the gripper, the gripper/object contact area is very small but the substrate contact area is unchanged. One can then expect a higher adhesion to the substrate. The key component for this release mode is hence the control of the contact force.

III. The manipulator

The micromanipulation system developed in our lab is built around an active gripper, whose design is based on the adhesion phenomena. According to the study presented above, it includes two important capabilities: high acceleration generation for dynamical release and precise contact force control for rolling. This gripper is an AFM (atomic force microscopy) tipless probe, mounted on a piezoelectric ceramic which can produce impulses or high frequency sinusoidal waves, generating instantaneous accelerations as high as 10^6 ms^{-2} at the extremity of the AFM cantilever. These outstanding dynamical capabilities are used for release and characterization tasks. The gripper also provides micronewton resolution measurement of the contact force, due to the AFM probe. Its vertical displacement is provided by two serial actuators: a nanostage with $12\,\mu m$ amplitude and a microstage with sub micrometer resolution over $2.5\,cm$. The contact force can thus be controllod by the motion of these actuators. The horizontal motion is produced by two identical microstages on $X-Y$ plane. Fig. 2 shows the whole micromanipulator, called [*mü*]MAD, placed under an optical microscope. The active gripper is shown in Fig. 3.

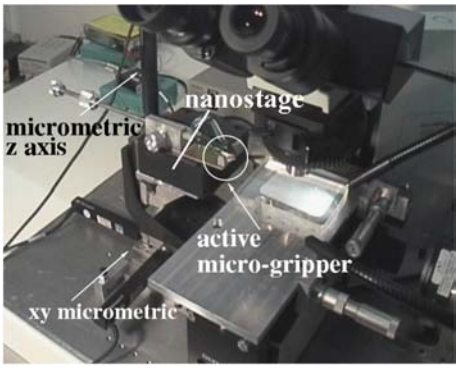

Fig. 2. The micromanipulator [*mü*]MAD

In order to control the overall motion of the manipulator, an interface with at least 3 DoF is needed. The chosen one is Virtuose 6D from Haption (*www.haption.com*, Fig. 4). It is 6 DoF 6R arm with its own computing resources, in order to reduce the CPU load of the workstation. It

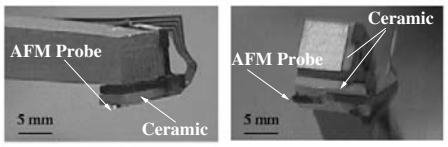

Fig. 3. The active gripper

is internally controlled on force or position, with inertial and mass compensation. This control also includes inverse geometric and dynamic models, so it can easily be controlled from an external application by sending set-point positions or forces. Its characteristics are given in Table I.

TABLE I
SPECIFICATION OF THE VIRTUOSE 6D MASTER DEVICE

Geometric characteristics	
Maximal stroke	45 cm
Dynamic characteristics	
Maximum effort F_{macro}^{max}	35 N
Overall	
Appearing mass M_{Virt}	1 kg
Appearing inertia I_{Virt}	0.03 kgm^2

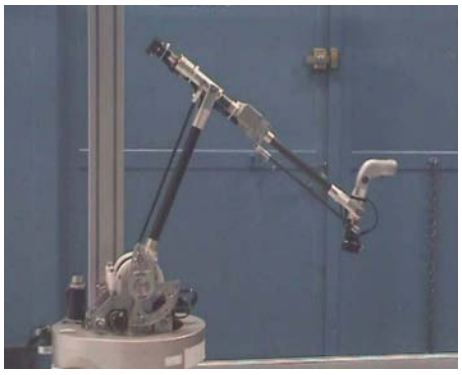

Fig. 4. Virtuose 6D haptic arm

IV. Control implementation

For autonomous manipulation and user assistance, vision and force servoing are implemented in [*mü*]MAD. For horizontal plane motion, visual servoing based on the microscope top-view is used. For the vertical motion, due to the very small depth of field of microcope image, a focus-based control is implemented. Force control uses the grippers measurement capabilities with both vertical actuators, the nanostage and the microstage and takes advantages of this intrinsic redundancy.

A. Motion of the gripper on horizontal plane

Position servoing of the gripper in the horizontal plane is done by image-based visual servoing using an external camera, described by Fig. 5. The gripper is detected by template matching in the microscope image and a desired contact point is defined by the user by clicking in the

image.The goal is then to reduce the error $(\epsilon_x\ \epsilon_y)$ between the gripper contact point desired position $(u^*\ v^*)$ and its actual position $(u\ v)$ in the current image (i.e. expressed in *pixel coordinates*) by appropriately moving it in the workspace.

Even if the static error of this servoing is null, there is a remaining uncertainty about the absolute position of the gripper, which depends on the real area size covered by a pixel (i.e. on the zoom). In our case, this uncertainty is about $2\mu m$, which is not very accurate, but it is now stabilized with respect to the vertical motion. Indeed, if the optical and motion axes are not perfectly aligned, the induced deviation is permanently corrected. (For an alignment error of 1 degree and a vertical motion of $1mm$, the gripper would deviate by more than $17\mu m$.)

B. Focusing for vertical motion

The goal of an autofocus algorithm is to find the appropriate camera position so that a part of the image is focused. Moreover, as the vertical camera motion is precisely controlled, it can be used to measure the vertical gap between different features in the image and hence control the vertical gripper motion. Focus perception is not an absolute criterion. However, some image properties are affected by good or bad focus and can be used to build suitable criteria. Among these observations, we can say that focused images have more high frequency components, more localised histograms, higher contrast, higher peaks and deeper valleys than blurred images. With a criterion based on one of these properties, the focusing problem can be processed as an optimisation problem.

Some simple criteria have been tested, the chosen one being to quantify high frequency components of the image. For an image I_z, taken by camera at position z, of width N and height M, the criterion is written as

$$f(z) = \frac{1}{NM} \sum_{i=1}^{N-2} \sum_{j=1}^{M-2} \sqrt{|G_x(i,j)|^2 + |G_y(i,j)|^2}, \quad (2)$$

where G_x and G_y are the convolution of the initial image I_z with respectively horizontal and vertical Sobel masks

$$S_x = \begin{bmatrix} -1 & 0 & 1 \\ -2 & 0 & 2 \\ -1 & 0 & 1 \end{bmatrix} \quad \text{and} \quad S_y = \begin{bmatrix} -1 & -2 & -1 \\ 0 & 0 & 0 \\ 1 & 2 & 1 \end{bmatrix}.$$

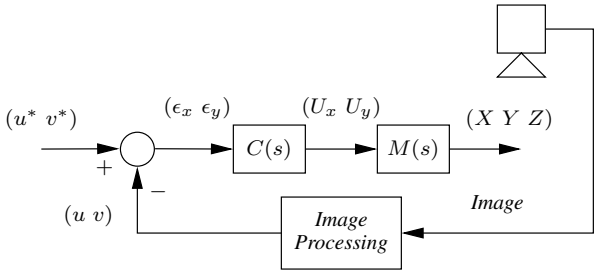

Fig. 5. Image based visual servoing scheme

Fig. 6 illustrates a measure of focus versus camera position, using the described criterion.

Note that f is null for blurred images. In this case, the camera is driven in constant speed. When the criterion becomes non null, the desired camera motion speed is computed as:

$$v_c^* = K \Delta_n f \quad (3)$$

where K is the gain and $\Delta_n f$ is the average slope of f computed on the last n measures.

C. Force servoing

As the AFM probe supplies only the measurment on the vertical axis, the force control is implemented for the vertical motion of the gripper through two redundant actuators, as described in Table II. The given induced force resolution is theoretical because it is only computed from the travel range resolution.

1) Basic loop: A basic force servoing loop has been implemented to control the nanostage, thus the gripper is able to apply a precise contact force. Figure 7 shows the force control scheme. F^* and F are the desired and measured force, ϵ_n is the servoing error, U_n the input voltage and, z_n the nanostage position, $N(s)$ the transfer function of the low level controlled nanometric stage, $G(s)$ the transfer function of the beam and $C_n(s)$ the corrector term.

Since we use a proportional corrector, $C_n(s) = K_n$, and considering the gripper and object in contact, the transfer function of the system can be written as

$$H_f(s) = \frac{K_n K_g N(s)}{1 + K_n K_g N(s)}. \quad (4)$$

Owing to its travel range of $12\mu m$, the nanostage easily reaches its bounds. Hence, the gripper should be very close to the object (a few micrometers) before starting the servoing in order to keep as much travel range as possible. The position information given by focusing is not accurate enough to

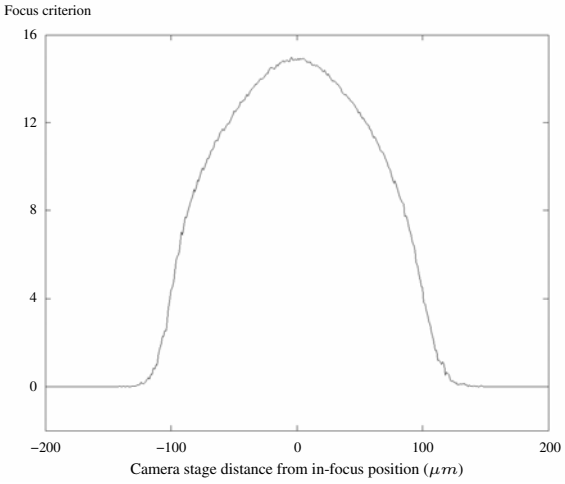

Fig. 6. Focus criterion measure

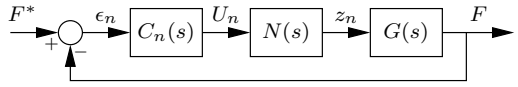

Fig. 7. Basic force servoing loop scheme

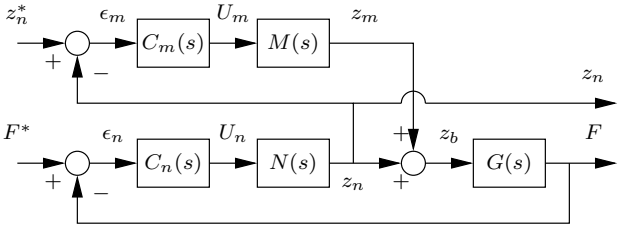

Fig. 8. Enhanced force servoing loop scheme

accomplish this operation. It is thus necessary to include the microstage in the force servoing loop.

2) Enhanced loop: An auxiliary loop controlling the microstage is associated with the basic one, whose goal is to maintain the nanostage in the middle of its travel range. Due to their different resolutions, it is important to define a dead zone around the desired nanostage position where the auxiliary loop has no effect in order to avoid undesirable oscillations. Fig. 8 illustrates the overall servoing scheme.

When a contact force F^* is desired, and the measured force F is null, the nanostage reaches its bottom bound due to the fast loop, and moves out of the dead zone. Consequently, the microstage moves down due to the auxiliary slow loop. When the gripper reaches the object, a non null contact force is measured and the former loop works in linear mode. The secondary loop will stop when the nanostage is in the dead zone and activate again if a new force command makes the nanostage go out of the dead zone.

V. Position-position bilateral coupling

The proposed control scheme is called position-position bilateral control. It will be hereafter referred as '*PPB*'. Its design is based on passivity considerations for teleoperated systems [10].

The architecture of the *PPB* control is modular. The global control is composed of three modules: the master control block, the homothetic coupling block and the slave control block (Fig. 9). The unconditional stability of the overall control scheme is guaranteed by ensuring that each block is stable by itself.

Parameters used in this control are given Table III.

TABLE III

System parameters

P_M,V_M	Measured position/velocity of master
F_{macro}	Force on master
P_{nano},V_{nano}	Measured position/velocity of nanostage
P_s, V_s	Set-point position/velocity of nanostage
P_{macro}, V_{macro}	Position/velocity of nanostage translated in macroworld
F_{canti}	AFM gripper measured contact force

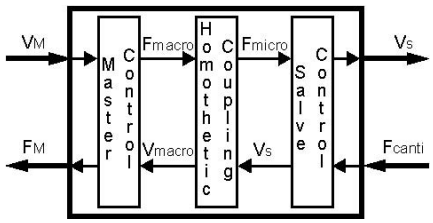

Fig. 9. The *PPB* control scheme decomposition

A. The homothetic coupling block

The homothetic coupling block is used for macro-to-micro and micro-to-macro conversions, between force F, position P and velocity V data, using force and motion scaling ratios α_f and α_d. Scaling ratio are defined according to the master used for the teleoperation, [*mü*]MAD and the desired performances. The motion of micromanipulator will be controlled by the haptic interface, thus the motion scaling is 'macro to micro'. On the contrary, the force is measured in the microworld and transmitted to the master haptic interface, thus the force scaling is 'micro to macro'.

Micro and macro homothetic ratios are thus defined as follows:

$$P_{macro} = \alpha_d P_{nano} \tag{5}$$

$$V_{macro} = \alpha_d V_s \tag{6}$$

$$F_{micro} = \alpha_f F_{macro} \tag{7}$$

B. The master control block

The master control block allows to compute the set-point force on the master F_{macro}, which is also used in the slave control block after using the force scaling ratio. It is a proportional-derivative control of the error on the master position with respect to the slave position converted into macroworld. In a two port model it has the velocity of the nanostage translated to macroworld V_{macro} and the velocity of the master V_M as inputs.

$$F_{macro} = K_p\left(P_M - P_{macro}\right) + K_d\left(V_M - V_{macro}\right) \tag{8}$$

with control parameters K_p and K_d chosen in accordance to the sampling period T_e.

Moreover, the damping ratio id is set as $\zeta = 1$ in order to limit the over-shooting.

$$\frac{2\zeta}{\omega_0} = \frac{K_d}{K_p} \Longrightarrow K_d = \frac{2\zeta K_p}{\omega_0} \tag{9}$$

TABLE II

Vertical axis specification

Axis type		Micro	Nano
Travel range	(μm)	2510^3	12
Travel resolution	(nm)	50	2
Induced force range	(μN)	526.510^3	252.72
Induced force resolution	(nN)	$1.053\ 10^3$	42.12
Loop period limitation	(ms)	40	-

C. The slave control block

The slave control block allows to compute the set-point velocity V_s of the nanostage, which is also sent back to the homothetic coupling block to be used in the master control. The calculation of V_s is based on the comparison of the master force translated in the micro world F_{micro}, and the cantilever contact force F_{canti} as in (10). As the nanostage is controlled on position, P_s is computed by integrating V_s with saturation levels at 0 and $12.10^{-6}m$, travel limits of the nanostage.

$$V_s = K(F_{micro} + F_{canti}) \tag{10}$$

where K is the enslaving gain. Simulations show that good performances are achieved with $K = 3$.

Note that in this case only the nanostage is coupled to the haptic interface. For complete coupling of both micro and nanostages, the slave control block is replaced by the enhanced force control loop presented in IV-C.2.

The passivity of this control scheme is studied using Llewellyn criteria [11]. This study has concluded to the unconditional stability of the overall system as all 3 Llewellyn criterion are verified independantly of chosen homothetic scaling ratios.

VI. Experiments

A. Adhesion forces

A glass sphere of $50\,\mu m$ in diameter lying on a polystyrene substrate has been captured by simple contact with the gripper (Fig.10). The estimated adhesion forces on substrate/object and gripper/object interfaces are respectively $F^{so}_{adh} = 4.70\ \mu N$ and $F^{go}_{adh} = 6.80\ \mu N$.

(a) Approach (b) Adhesion (c) Capture

Fig. 10. Capture by adhesion of a $50\mu m$ diameter object

1) Dynamic effects: In this second example, the capture operation is achieved by adhesion, as in the previous case. The release task on the contrary is accomplished by inertial effect. The necessary acceleration to produce this inertial force is estimated around $10^6\ m/s^2$. This acceleration can be reached by exciting the piezoceramic actuator with a $120\,V$ $1\,\mu s$ impulse. The fig 11 shows the output signal of the AFM device for this case.

This output signal is proportional to the inflection of the AFM cantilever. The high magnitude of the impulse causes important vibrations of the AFM cantilever, as observed on the output signal.

A change of the oscillation frequency of the cantilever is visible at $t = 150\,\mu s$. After this instant, the cantilever oscillates at $40\,kHz$, which is its first free inflection mode of the cantilever alone. We can deduce that the object adheres to the gripper until this instant, and is then released, changing the natural frequency of the system. It is then possible to judge the release by mere observation of the output signal of the AFM, without needing any other external sensor.

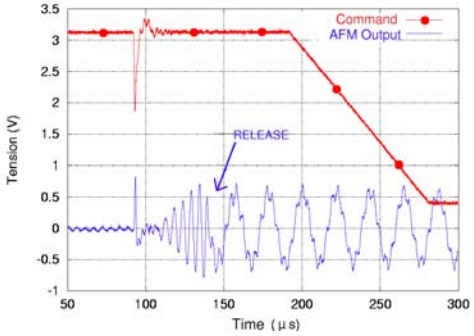

Fig. 11. Dynamic release of a $40\mu m$ radius glass sphere

The dynamic mode, as described in this example, allows to release the captured object independently of external factors, such as the geometry of the object or the target substrate.

B. Sorting by selective release

The selective release is an extension of the dynamic release mode by use of vibrational behavior of the AFM cantilever. Ambrosia pollens, approximately $20\,\mu m$ in diameter are introduced. These specimens come in powder and they form a very dense and homogeneous distribution on the substrate. It is quite difficult, if not impossible, to pick an isolated pollen. Thus, in the approach-and-capture cycle, several pollens are captured. We report an experiment with 2 pollens caught. In order to release those objects, the piezoceramic actuator is excited with a sinusoidal signal with frequency variation. As the pictures of Fig. 12 illustrate, it is then possible to release the objects captured in random one by one.

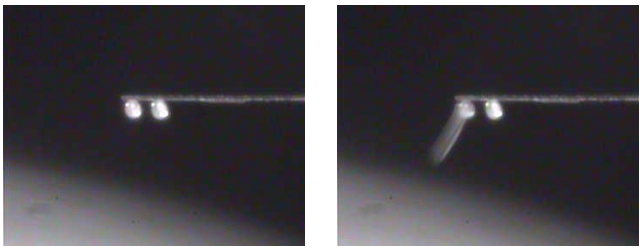

(a) Release of the first object

(b)Release of the second object

Fig. 12. Selective release operation

This operational mode basically allows to isolate a micro-object from an initial large group.

C. Teleoperation

[*mü*]MAD is also experimented in teleoperation using the proposed *position-position* coupling, which was compared to a basic force-position coupling scheme. Pick-up, rolling and release operations of ragweed pollens (diameter=20μm) are experimented (Fig. 13). During this experiments, users is perfectly able to feel stiffness of the pollens when compressed and rolled, as well as the pull-off and adhesion forces during release. *Position-position* coupling shows better performances such as the feeling of the bounds and the damping coefficient between the master and the slave. Fig. 14 illustrates the master's position vs. nano and microstage motions. Moreover, it is even possible to change the scaling ratios on the fly (under some restriction on energy dissipation), as the stability of the system is unaffected. It is then possible to adapt the coupling to a given phase of the manipulation task which would need more or less precision or travel range using the same haptic interface.

VII. Conclusion

In this paper, advanced functionalities of [*mü*]MAD, the adhesion-and-dynamics micro-manipulator are presented. The system is capable of capturing micro-objects smaller than a few micrometers, based on the superiority of adhesion forces for this class of object. The release is accomplished either by adhesion, on a higher energy target substrate, or by amplification of inertial force by way of an instantaneous acceleration applied to the gripper. Furthermore, important dynamic performance of the gripper and a controlled vibrational behavior of the AFM cantilever used as end-effector allow some interesting applications, such as the selective release or measurements on the mechanical characteristics (mass, stiffness) of manipulated objects. Moreover, enhanced

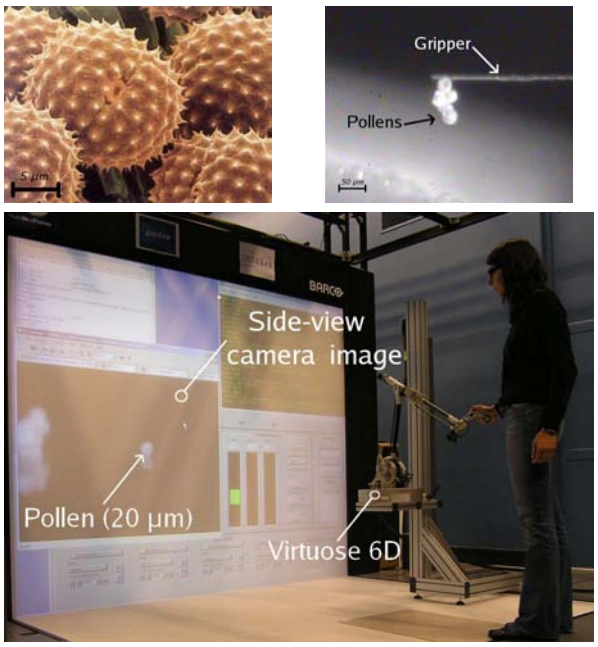

Fig. 13. Manipulation of ragweed pollens

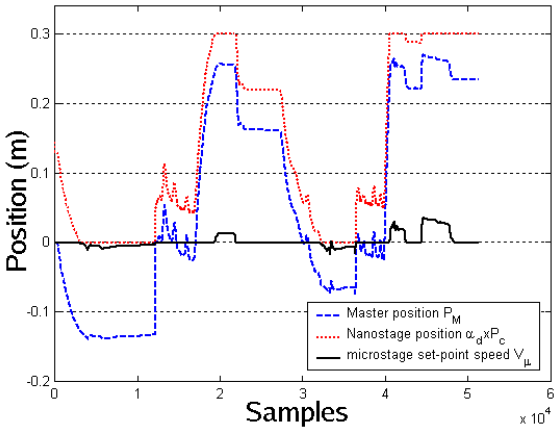

Fig. 14. Results using the Virtuose 6D as master

user interaction is provided via a force-feedback haptic interface. This setup permits a very intuitive access to micro-world and opens the way for easy integration of user-guided micro-manipulation, for MEMS assembly process as well as for biological applications.

References

[1] S. Saito, H. Miyazaki, and T. Sato, "Micro-object pick and place operation under sem based on micro-physics," *Journal of Robotics and Mechatronics*, vol. 14, no. 3, pp. 227–237, 2002.

[2] F. Arai, A. Kawaji, P. Luangjarmekorn, T. Fukuda, and K. Itoigawa, "Three-dimensional bio-micromanipulation under the microscope," in *Proc. of the International Conf. on Robotics and Automation Vol. 1 (ICRA 2001)*. IEEE, 2001, pp. 604–609.

[3] Y. Rollot, S. Haliyo, S. Régnier, L. Buchaillot, J. Guinot, and P. Bidaud, "Experimentation on micromanipulation using adhesion forces in unconstrained environment," in *proc. of the IEEE/RSJ International Coference on Intelligent Robots and Systems (IROS2000), Japon, october 2000*, 2000, pp. 653–658.

[4] D. Haliyo and S. Régnier, "Manipulation of micro-objects using adhesion forces and dynamical effects," in *Proceedings of ICRA/IEEE International Conference on Robotics and Automation*, May 2002.

[5] F. Dionnet, D. Haliyo, and S. Rgnier, "Autonomous micromanipulation using a new strategy of accurate release by rolling," in *sProceedings of ICRA/IEEE International Conference on Robotics and Automation*, 2004.

[6] J. Israelachvili, *Intermolecular and Surface Forces*. Academic Press, 1991.

[7] Y. Rollot, S. Regnier, and J.-C. Guinot, "Dynamical model for the micromanipulation by adhesion : Experimental validations for determined conditions," *International Journal of MicroMechatronics*, vol. à paraitre, 2000.

[8] K. Johnson, *Contact Mechanics*. C.U.P. Edition, 1985.

[9] B. V. Derjaguin, V. Muller, and Y. P. Toporov, "Effect of contact deformations on the adhesion of particles," *Journal of Colloid and interface science*, vol. 53, No. 2, pp. 314–326, 1975.

[10] R. J. Adams and B. Hannaford, "Stable haptic interaction with virtual environments," *IEEE Trans. on Robotics and Automation*, vol. 15, no. 3, pp. 465–474, 1999.

[11] R. Adams and B. Hannaford, "A two-port framework for the design of unconditionally stable haptic interfaces," in *Proceedings of IROS*, 1998, pp. 1254–1259.